Naval Research Laboratory
Washington, DC 20375-5320

NRL/MR/6180--03-8682

The Effects of Air-Borne Water Mist on a Forced Convection Boundary Layer Flame Over a Non-Charring Solid

CHUKA C. NDUBIZU

Geo-Centers, Inc.
Lanham, MD

RAMAGOPAL ANANTH

Navy Technology Center for Safety and Survivability
Chemistry Division

PATRICIA A. TATEM

Global Paperless Solution
Alexandria, VA

May 30, 2003

REPORT DOCUMENTATION PAGE

Form Approved
OMB No. 0704-0188

1. REPORT DATE *(DD-MM-YYYY)*	2. REPORT TYPE	3. DATES COVERED *(From - To)*
May 30, 2003	Memorandum report	

4. TITLE AND SUBTITLE

The Effects of Air-Borne Water Mist on a Forced Convection Boundary Layer Flame Over a Non-Charring Solid

5a. CONTRACT NUMBER

5b. GRANT NUMBER

5c. PROGRAM ELEMENT NUMBER

6. AUTHOR(S)

Chuka C. Ndubizu,* Ramagopal Ananth, and Patricia A. Tatem†

5d. PROJECT NUMBER

5e. TASK NUMBER

5f. WORK UNIT NUMBER

7. PERFORMING ORGANIZATION NAME(S) AND ADDRESS(ES)

Naval Research Laboratory
4555 Overlook Avenue, SW
Washington, DC 20375-5320

8. PERFORMING ORGANIZATION REPORT NUMBER

NRL/MR/6180--03-8682

9. SPONSORING / MONITORING AGENCY NAME(S) AND ADDRESS(ES)

Office of Naval Research
800 North Quincy Street
Arlington, VA 22217

10. SPONSOR / MONITOR'S ACRONYM(S)

11. SPONSOR / MONITOR'S REPORT NUMBER(S)

12. DISTRIBUTION / AVAILABILITY STATEMENT

Approved for public release; distribution is unlimited.

13. SUPPLEMENTARY NOTES

*Geo-Centers, Inc., Lanham, MD
†Global Paperless Solution, Alexandria, VA

14. ABSTRACT

This report presents preliminary results of an experimental study of water mist suppression of forced flow boundary layer flames over a non-charring solid, where fine water mist was introduced with the incoming air. In this configuration, extinguishment at high mist flow rates is achieved only by flame blow-off. With small droplets (~50 μm) at low mist flow rates, the time-averaged local burning rate seems to be suppressed in the leading section and enhanced downstream. A comparison of the burning rate and temperature data between tests with mist and tests with nitrogen dilution suggest that this enhancement in burning rate is caused by mist-induced turbulence.

15. SUBJECT TERMS

Fire suppression; Water mist

16. SECURITY CLASSIFICATION OF:			17. LIMITATION OF ABSTRACT	18. NUMBER OF PAGES	19a. NAME OF RESPONSIBLE PERSON
a. REPORT	b. ABSTRACT	c. THIS PAGE			Ramagopal Ananth
Unclassified	Unclassified	Unclassified	UL	27	19b. TELEPHONE NUMBER *(include area code)* (202) 767-3197

Standard Form 298 (Rev. 8-98)
Prescribed by ANSI Std. Z39.18

CONTENTS

Preceding Page Blank

The Effects of Air-Borne Water Mist on a Forced Convection Boundary Layer Flame Over a Non-Charring Solid

1.0 INTRODUCTION

Recent research in water mist fire suppression has been driven by two factors. First there is the need to find an environmentally friendly alternative to halogen-based agents, which have been shown to have adverse effects on the atmospheric ozone layer. Secondly, there is the need to meet the International Maritime Organization's regulation, which requires the replacement of sprinkler systems aboard commercial ships with low-weight systems. Water mist system is a contending technology for meeting these requirements. However water is a multiphase agent and therefore its transport and distribution imposes additional challenges, which limits its effectiveness. In fires involving condensed fuels (solids and high latent heat liquids) water mist is particularly effective if the droplets can get to the condensed fuel surface, where they absorb latent heat and evaporate. In this way the surface is cooled directly and the burning rate is suppressed rapidly.

Water mist systems have been chosen to replace Halon 1301 in the machinery space in the Navy's LPD-17 ship. There is need to develop a better understanding of the role of the various water mist fire suppression mechanisms to enable the Navy to expand the use of water mist systems to other spaces in future war ships. Previous studies of water mist fire suppression mechanisms and the transport/distribution challenges that affect water mist effectiveness were conducted mainly in co-flow fire configurations and these will be reviewed next. Boundary layer type flames are prevalent in bulkhead fires and wind-driven fires on aircraft carrier decks. However, we lack detailed studies of the transport/distribution effectiveness of water mist in laboratory-scale boundary layer flames, where the role of the various suppression mechanisms can be unraveled. This report focuses on the effects of air-borne fine water mist on the burning characteristics of a small-scale boundary layer flame.

1.1 Literature Review

The earliest studies of water mist fire suppression mechanisms were conducted by Rasbash and coworkers [1-3] in the co-flow configuration. They studied the extinction of 30-cm liquid pool fires with water mist and outlined the mechanisms of water mist suppression of fires. Their results reveal that as the droplets evaporate in the combustion zone the water vapor dilutes the oxygen concentration and absorbs additional sensible heat as it is heated to the fire temperature. The net effect of these processes is the suppression in fire gas temperatures (gas phase cooling). Some of the droplets may survive as they pass through the hot combustion region and eventually reach the condensed fuel surface. The droplets absorb latent heat from the surface to evaporate completely. This cools the surface, thereby reducing the gaseous fuel production rate.

Downie et al. [4] studied the suppression of a large methane pool fire subjected to a steady water mist spray from a single hollow cone nozzle mounted above the fire. The large plume-to-flame thrust ratio in their experiment resulted in negligible direct penetration of the droplets into the fire region. Their result shows a significant reduction in oxygen concentration and increase in carbon monoxide concentration inside the flame when the mist was applied. Takahashi [5] studied the extinquishment of plastic fires with

Manuscript approved April 28, 2003.

water spray. He compared extinquishment times with plain water and 'wet' water. Wet water is foam agent diluted 10,000-fold with water. He showed that wet water reduced the extinquishment time by as much as 50%.

McCaffrey [6] studied the suppression of a hydrogen jet diffusion flame by water mist in a co-flow arrangement. Experiments were run with sprays of small droplets introduced with the hydrogen jet. They were interested in the feasibility of using water sprays to control off shore oil/gas blowout. Their results show a strong correlation between the suppression in flame temperature and the mist droplet size, which reveals that smaller droplets will be more effective in fighting oil/gas blowout fires.

Detailed numerical models of the interaction of water spray with fires in the co-flow configuration have been reported by other workers. Alpert [7] developed a field model to predict the penetration of a sprinkler spray through the plume of a burning object. The model essentially combines a model of a 2-D flow produced by a heated jet (or ordinary heat source) and a water spray model. Later, Bill [8] verified this model using the Factory Mutual Research Corporation's actual delivered density (ADD) apparatus. Their results show some good agreement between the predicted and measured density of water reaching the base of a heptane spray fire when the sprinkler nozzles are located 3.05m and 4.57m above the base.

Prasad et al. [9-11] developed a numerical model to study the interaction of water mist spray and a small laminar 2-D diffusion flame. The model combined a fire model and a spray model to predict temperature and species profiles in the suppressed flame. In co-flow injection of water mist their model predicted that smaller droplets get entrained into the flame more easily and are more effective than larger droplets. Later, a parametric study [11] was undertaken where the droplet size, velocity, number density, spray orientation (base, top or side) and spray angle were varied. The results of this study show that optimum suppression is obtained with small droplets injected from the base, while larger droplets are needed for optimum suppression when droplets are injected from the sides.

We had studied [12] the contributions of the various water mist fire suppression mechanisms in a slot burner flame, where nitrogen, steam and water mist were injected in a co-flow arrangement. Our results show that the effects of thermal cooling are more significant than those of oxygen dilution in this configuration. Later we investigated [13] the effects of droplet size and injection orientation on water mist suppression of low and high boiling point 50-cm liquid pool fires. Our measurements show that optimum suppression effectiveness is obtained with small droplets injected at the base of the fire and that the effects of direct cooling of condensed fuel surface by evaporating water droplets are very significant.

The few studies on the effects of water mist in boundary layer fire configuration were interested in the extinguishment rather than suppression of the flame. Tamanin [14] investigated the extinguishment of a burning vertical plastic slabs by a horizontal water spray. He obtained a power-law correlation between the burning rate and the water application rate. Earlier, Magee and Reitz [15] conducted similar experiments, where

vertical and horizontal plastic slabs were subjected to turbulent burning with external radiation. They determined the critical conditions for extinguishment and showed that for plastics that do not melt excessively, the primary mechanism for suppression is by surface cooling.

In this work, we consider a small-scale horizontal PMMA slab burning under a forced convection boundary layer flame. We emphasize suppression rather than extinguishment, so that the effects of mist droplets at various locations in the flame can be studied. Unlike in the previous work, fine water mist is introduced with the airflow. The key objectives of this work are (i) to study the controlling mechanisms in water mist suppression of forced convection boundary layer flame and (ii) to determine the effects of key mist parameters (e.g. droplet size distribution) on the suppression effectiveness.

Earlier we had conducted detailed studies of the burning characteristics of the PMMA plate without mist (base case). The objective is to understand how the plate burns without mist so that the effects of mist interaction with the flame and PMMA plate can be deduced more accurately. The results of the base case studies [16,17] show that as the PMMA plate burns, the stream-wise surface profile become non-uniform and time dependent. We showed that the effects of this non-uniform surface profile and its change with time results in the follow:

- Transient local burning rate, with burning rate decreasing in the leading section and increasing downstream. We showed that the local burning rate depends not only on location and convective flow but also on burn time.
- Surface curvature-driven flame spread upstream into the quench zone, where the flame could not sustain when the surface was flat, molten and pyrolyzing. Our results reveal that the presence of a small valley near the leading edge of the flame stabilizes the flame, perhaps by creating a stagnation/re-circulating zone that increases the Damkholer number and enables the flame to spread upstream.

This report presents preliminary results of the effects of the introduction fine droplets (Sauter mean diameters (SMD) ~50μm) into the convection air. We will discuss the changes in the local burning rate and gas phase temperature profiles as a result of mist action.

2.0 EXPERIMENTAL

Figure 1 shows a schematic of the experimental setup, whose key components include the wind tunnel, the PMMA sample holder, an ATC® weigh platform and thermocouples mounted on a set of Velmex X-Y unislides. The wind tunnel has a 36 X 45 X 61 cm plenum at one end into which an Ametek RJ054 ® variable speed blower pumps air. Pressure build up in the plenum drives the flow of the oxidizer through the wind tunnel and hence the effects of the blower on the flow are minimized. A 30-cm converging section connects the plenum to the 120-cm straight section, which has a 15 cm X 15 cm cross section. A set of fine screens are placed at the entrance and exit of the converging section and a 3mm honeycomb, 2.5 cm thick is inserted 90 cm upstream from the tunnel exit to smooth the flow. The flow velocity in the wind tunnel is selected by adjusting the speed of the blower. Spray nozzles are used to inject mist into the airflow in

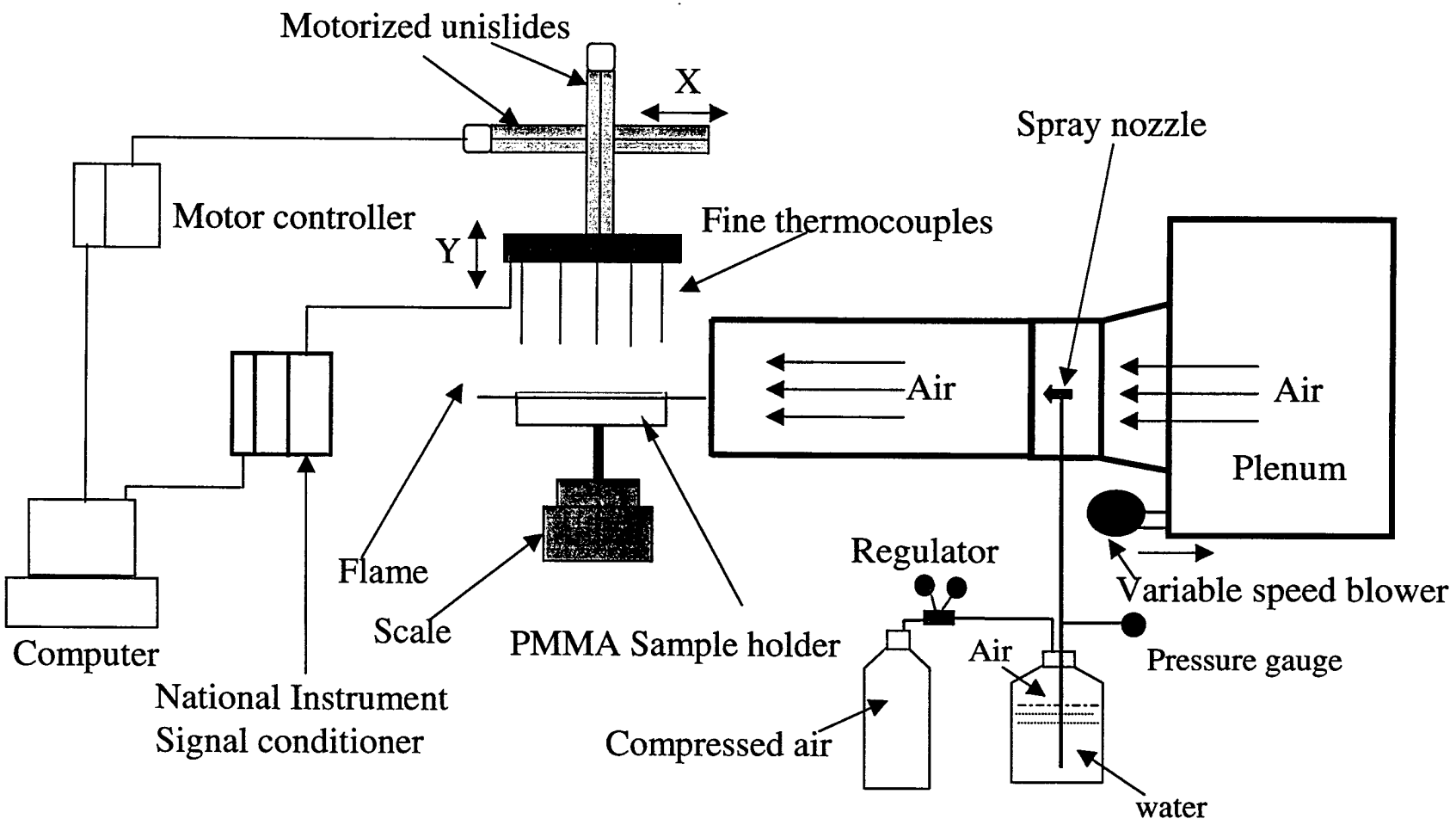

Figure 1: Schematic of the experimental setup

a 30-cm chamber at the beginning of the straight section. Distilled water in a ~ 9.4 liter tank is pressurized by compressed air and forced through a spray nozzle placed at the center the mist generation chamber (Fig. 1). A steady mist flow rate is obtained by keeping the pressure constant using a Matheson 3030® regulator. The mixture of air and water mist flows through the 15cm X 15 cm X 90 cm straight section to the exit of the tunnel, where the burning PMMA plate is located.

Generally, in forced flow boundary layer flame experiments, the fuel sample is placed inside a wind tunnel (e.g. McAlevy and Magee, [18]). In this work, we placed the PMMA sample at the exit of the wind tunnel at the center of the jet. This arrangement has two advantages. First, we have easy access to move thermocouples in and out of the boundary layer flame to map temperatures. Secondly, we avoid water dripping on the burning surface from the wind tunnel ceiling, which would taint the results. To ensure that the flow is well defined at the location of the flame, we chose the size of the sample and sample holder to be small such that the PMMA would be within the potential flow core of the exit jet. It has been shown [19,20] that the velocity profiles in both X and Y directions do not change significantly within the potential core of the jet. Furthermore, experimental measurements of Sforza et al. [21] show that for an air jet at the exit of a square channel, with Reynolds number Re_d between 2.6×10^4 and 8.8×10^4, the potential core length is about 5d downstream of the exit, where d is the height of the channel. In the current work, d = 15 cm and hence our sample is within 1d (14 cm from tunnel exit). Our Re_d is between 0.6×10^4 and 2.2×10^4 implying that the flame would be within the potential core of the exit jet.

Five R-type thermocouples, 50 μm (0.002") in diameter, are mounted on the Velmex® X-Y unislides. The unislide motors are computer controlled by a Velmex® NF90 controller such that the thermocouples can be placed precisely at any point in the middle plane of the flame. Voltage signals from the thermocouples go through National Instruments ® TC 2095 terminal block into the SCXI 2000 chassis where the signals are conditioned and digitized. LabView software is used for motor control as well as continuous temperature and weight data acquisition. Figure 2 shows a picture of the experimental setup.

The sample holder is made of a thin 1.5-mm-thick aluminum plate (18.5 cm x 19 cm) brazed onto a 10 cm x 8 cm x 2.1 cm deep cup, which holds the PMMA sample. The holder is designed to have a 4-cm rim in the leading section and a 5-cm rim in the other three sides. At the measurement location, the holder is positioned with its leading edge against the tunnel exit at the center of the channel (see insert in Fig 2). Since the rim is wider (18.5 cm) than the width of the tunnel (15 cm) the exiting air jet is divided into two and the top half forms a boundary layer over the sample.

Thin strips of quartz glass are placed between the PMMA sample and the walls of the holder on all the four sides to prevent molten PMMA from sticking on the walls of the sample holder. The sample holder sits on the ATC® weigh platform mounted on a slide mechanism such that the sample can be ignited under the radiant panel located about

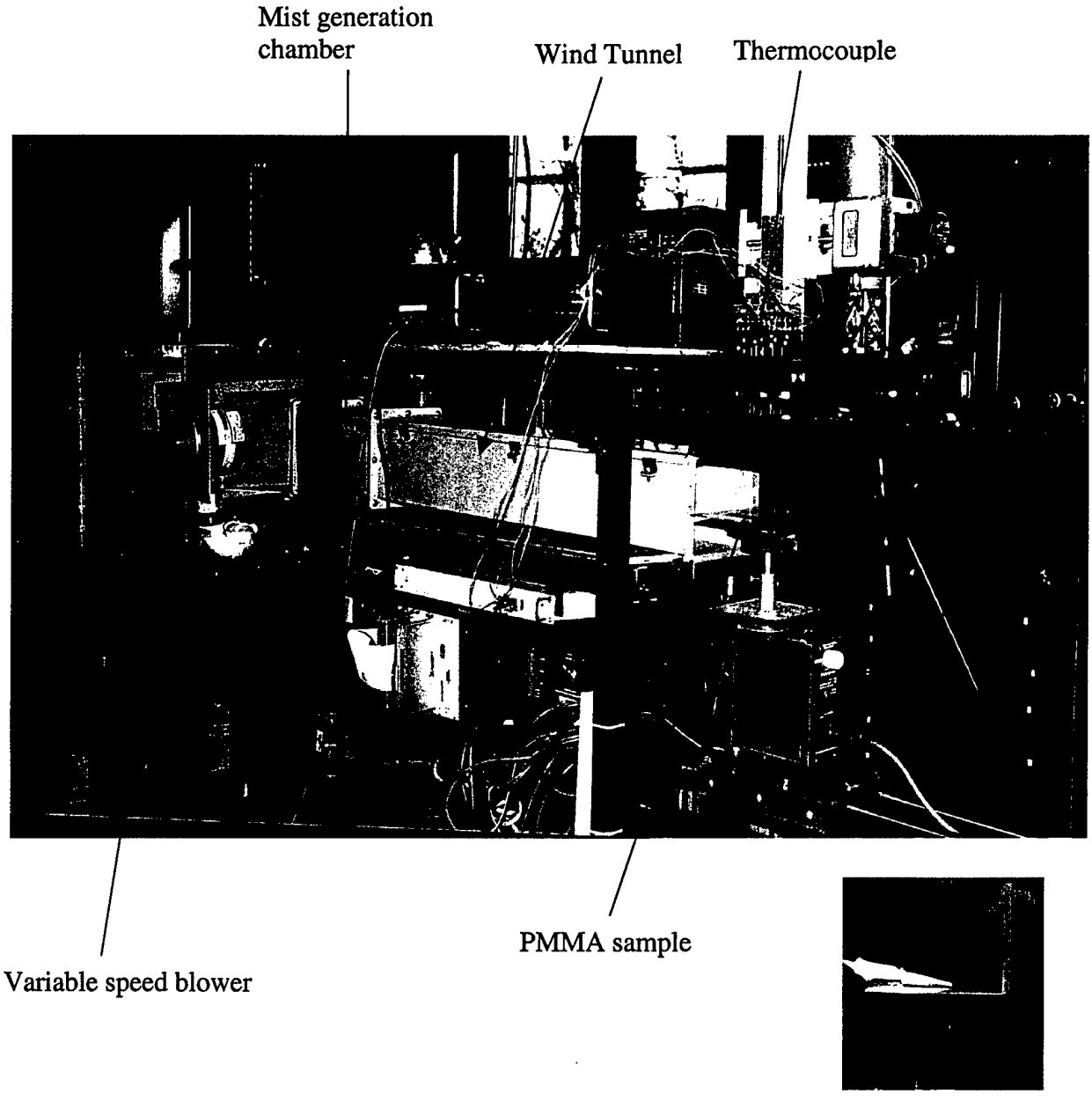

Figure 2 : Picture of the Experimental Setup. Insert: Picture of the flame at the tunnel exit.

40 cm downstream from the tunnel exit and quickly moved to the tunnel exit after ignition.

The 7.5 x 9.5 cm PMMA samples are made from Cyro® Acrylite GP sheet nominally 2.54 cm thick. The samples were milled to a thickness of 2.3 cm. The choice of sample thickness is influenced by the experiments of Vovelle et al. [22] and also Tewarson and Pion [23], which showed that the initial sample thickness does not affect the burning rate if it is larger than 1.5 cm.

2.1 Test Procedure

First, the nozzle is setup in the mist generation chamber and the air pressure is set in the water tank. The blower is turned on and adjusted to produce a U_∞ at the exit of the tunnel (measurement location) as measured by a hot wire anemometer. The velocity profile across the tunnel without mist is relatively uniform near the center. This uniform velocity is the free stream velocity U_∞. This report will present results with $U_\infty = 84$ cm/s.

In mist experiments, the mist is tuned on as the entire sample surface is uniformly heated under a radiant panel and ignited (Fig. 3). The process of irradiation, surface gasification and the establishment of a stable 2-D flame over the sample, take place in about 40 seconds. Time is started immediately after ignition. Thereafter, the burning sample is quickly moved to the measurement location at the tunnel exit. Gas phase temperatures are measured simultaneously at five X locations with five thermocouples. The sample is allowed to burn for a known time interval before the flame is extinguished. The mist flow is then turned off. After the sample cools down, its thickness along the centerline is measured at various X locations with a digital micrometer whose accuracy is ±0.003 mm. Since the initial thickness of the sample was measured, the sample regression rate at each location is obtained as the difference in thickness, after correction for PMMA thermal expansion [24] divided by the test duration. This report presents results of tests that lasted for 10 minutes.

2.1.1 Temperature measurement

As the PMMA sample burns, its surface regresses with time and the flame moves down accordingly. Although surface regression is not uniform along the sample length, the highest regression rate (near the leading edge) is ~ 1 mm/min. If the flame moves down at that rate, it is necessary to complete the temperature mapping across the flame in under 1 min to avoid significant errors in the measurement. At the same time it is necessary to allow enough time (≥ the thermocouple time constant) during each measurement for the thermocouple bead to attain thermal equilibrium with the surrounding gases. For a 50 μm diameter thermocouple the bead diameter (butt-welded) is about 125 μm and the time constant is approximately 30 ms [25]. Since the temperature gradient is very large within the boundary layer, measurements need to be made at very short distance intervals. The boundary layer is ~ 10 mm in the trailing section and twenty measurements at 0.5 mm intervals were made across the flame at each X location to map the temperature within the boundary layer. To meet these requirements

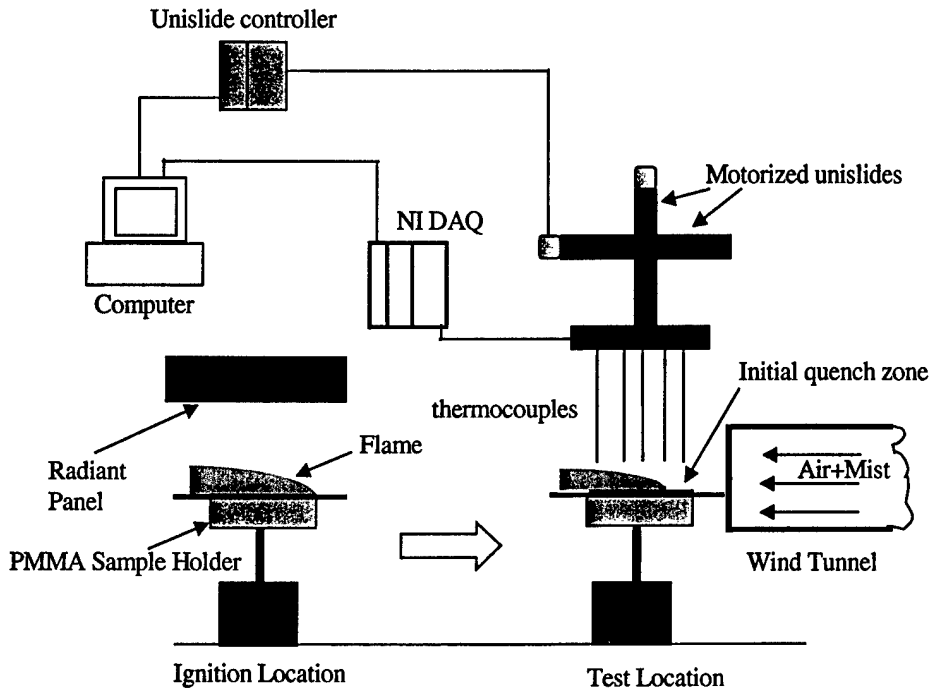

Figure 3: Schematic of the process of establishing a stable flame

and acquire the data in order of 1 minute, the data acquisition system was programmed to acquire data at the rate of 20 per second and 20 samples were averaged per recorded data. However, to avoid mist accumulation on the thermocouple beads and possible dripping on the flame, the thermocouples are withdrawn outside the reach of the mist stream (above the tunnel opening, Fig. 2). Hence the thermocouples have a long travel (>6.5 cm) before they reach the measurement area. With the travel time of the thermocouple and the processing time, the temperature mapping across the entire flame was completed within 80 seconds.

Since the thermocouples were crossing regions of high temperature gradients, the measurements are expected to include conduction errors. To minimize this error we chose very fine thermocouples with diameter of 50 μm. The conduction error with these thermocouples is expected to be small since the heat transfer area (the cross sectional area of the thermocouple) is very small. No corrections were made in the data for conduction error. However, the temperature values are corrected for thermocouple bead radiation loss and the details about the correction are given elsewhere [12]. For the 50-μm-diameter thermocouple a typical radiation correction at 1800 K is +62 K

2.2 Mist Generation

The experimental setup was designed such that various mist generating systems (e.g., spray nozzles, ultrasonic mist generators) can be used to inject mist into the air stream. The results in this report were obtained with spray nozzles. Two sets of nozzles were used to obtain a wide range of droplet characteristics (diameter, number density). One set is the Spray Systems® Cold Fog Nozzles (CFN) with orifice diameters, d, of 0.004" (CFN4), 0.0045" (CFN45), 0.005" (CFN5) and 0.006" (CFN6). This corresponds to 0.1 mm ≤ d ≤ 015 mm (Fig. 4a) The other set is the Delavan® WDB nozzles with 60 degree spray angle and orifice diameters 0.21 mm ≤ d ≤0.33 mm (Fig. 4b). Generally the CFNs have lower flow rates and require higher pressures. With the d =0.1 mm (CFN4) nozzle, at pressures less than 400 psi, the mist flow rate from a single nozzle is too low to produce measurable effects. In that case two or more nozzles can be put together as shown in Fig. 4c.

The manufacturer provided the mist outputs of the CFN nozzles at high pressures (>400 psi). At low pressures, we measured the nozzle outputs by spraying the mist into a dry container for a known time and calculating the flow rate as $(\Delta\text{weight/time})\rho_w$, where ρ_w is the density of water. The nozzle outputs at low pressures as well as outputs at high pressures provided by the manufacturer are presented in Fig. A1 in the Appendix.

Droplet characteristics are to be measured dynamically without the flame at the flame location. We plan to make detailed measurements at three locations across the height of the mist cloud, namely, at the leading edge, middle and trailing edge of the sample. These measurements will be made with Malvern Instruments' Spaytec®, which is currently on order.

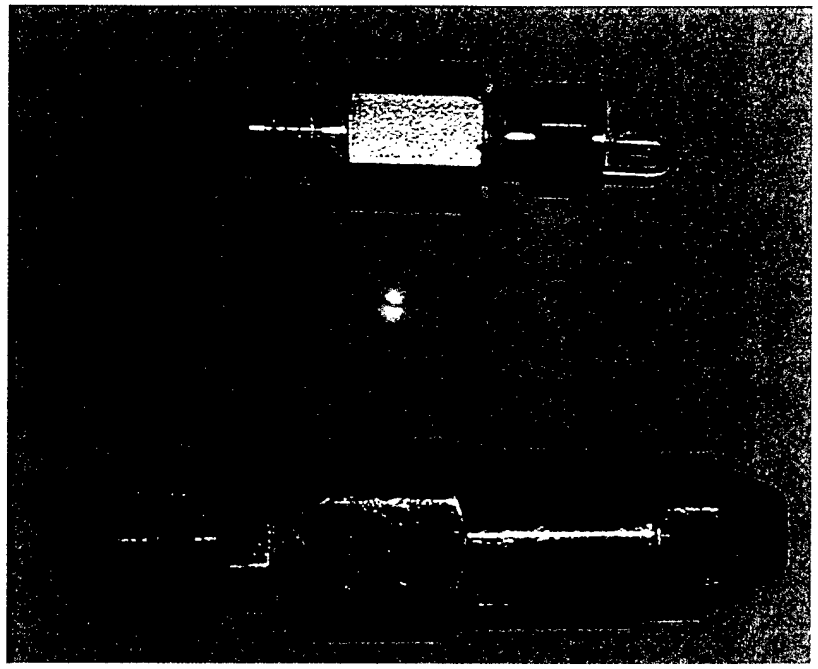

a

b

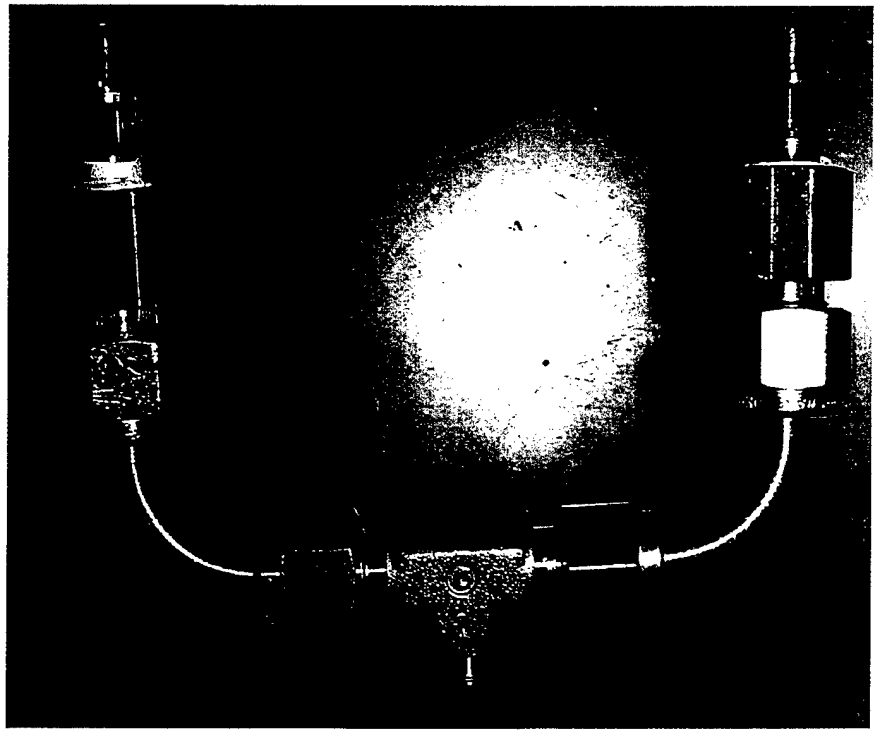

c

Figure 4: Picture of Spray nozzles used in the tests – (a) Cold Fog nozzle; (b) WDB nozzle; (c) Arrangement of two cold fog nozzle for higher mist flow

3.0 RESULTS AND DISCUSSION

The mist and airflow are turned on before the flame is ignited under a radiant panel, which is 40 cm downstream from the tunnel exit. At ignition the flame is anchored at the sample leading edge (Fig. 3). The burning PMMA plate is then moved to the tunnel exit, where the velocity of the mist-laden air is higher. Mist droplets evaporate in the flame and suppress the flame temperature and burning rate. If the mist flow rate is very high, the flame is dislodged at the PMMA leading edge and eventually blown off. In this case the Damkholer number (Da) is too low within the measurement location and the flame could not sustain. Several attempts were made to obtain stable flames under such conditions but in each case the flame was extinguished by being blown off. Thus flame extinguishment under these conditions is obtained by the creation of instability, dislodging the leading edge and eventual blow-off. Fig. 5a shows a picture of a flame being blown off because the mist flow rate is too high. It is interesting to note that the PMMA surface is still flat as the flame is being blown off. As we reduced the mist flow rate by lowering the water pressure, the flame only retreats from the leading edge and stabilizes downstream, establishing a quench zone, where the Da is too low for stability (Fig. 5b). As the surface curvature changes near the flame front, the flame creeps slowly upstream, decreasing the quench zone with time. In an earlier paper [17] we showed that this unusual flame spread is caused by the non-uniform surface regression, which is characteristic of the boundary layer combustion of PMMA. In some tests the flame could not spread up to the leading edge during the 10 minutes of the experiment. Figure 6 shows the surface profiles of three 10-minute tests. Figure 6a is the profile for the base case test, where the flame was anchored at the sample leading edge throughout the 10 minutes, while Figs. 6b& c are the profiles for tests with two CFN4 nozzles ran at 300 psi. and WDB1 nozzle ran at 50 psi. In the last two cases the flame had not spread up to the leading edge within the 10 minutes.

We present preliminary results with two Cold Fog nozzles (CFN4 and CFN6) ran at water pressures of 300 and 75 psi., respectively and three Delavan nozzles (WDB1.5, WDB1 and WDB05), ran at water pressures of 40, 50 and 100 psi., respectively. The free stream air velocity (U_∞) in these tests was 84±1 cm/s. and the burn time was 10 minutes. A full characterization of the droplets, in terms of droplet diameter distribution and concentration will be done soon. Table 1 shows preliminary characterization data measured at the middle of the channel without the flame with the Dantec ® Particle Dynamics Analyzer. The data in Table 1 are meant to give an indication of the range of droplet diameters used in these tests. With U_∞ = 84 cm/s the Suater mean diameter of the droplets in these tests are in the range of 50 μm.

Figure 7 shows a comparison of the measured local regression rates at various stream-wise locations in tests with and without mist. The solid symbols are the base case (BC) data while the open symbols are the various mist case data. Figure 7 show that in the leading section (X≤ 10 mm), the local burning rate is suppressed by the presence of water mist, however downstream (X > 20 mm) water mist seems to enhance the burning rate. The base case experiment was repeated a few times to show the scatter in the data. The peak regression rate in the leading section is suppressed by ~ 20% due to presence of water mist. The suppression in the leading section is a result of the formation of the quench zone in this section because of the high cooling effects of the mist. The length of the initial quench zone varied from about 3 mm to about 25 mm in these

Table 1:Mist Characteristics measured with Dantec PDA at the exit of the wind tunnel with air flow velocity of 84 cm/s.

Nozzle Type	Water Pressure (psi)	Droplet sauter mean diameter (μm)	Droplet concentration (#/cc)	Droplet mean velocity (cm/s)
2_CFN4	300	24.3	11426	87.3
CFN6	75	53.0	703	79.2
WDB1	50	51.8	529	106

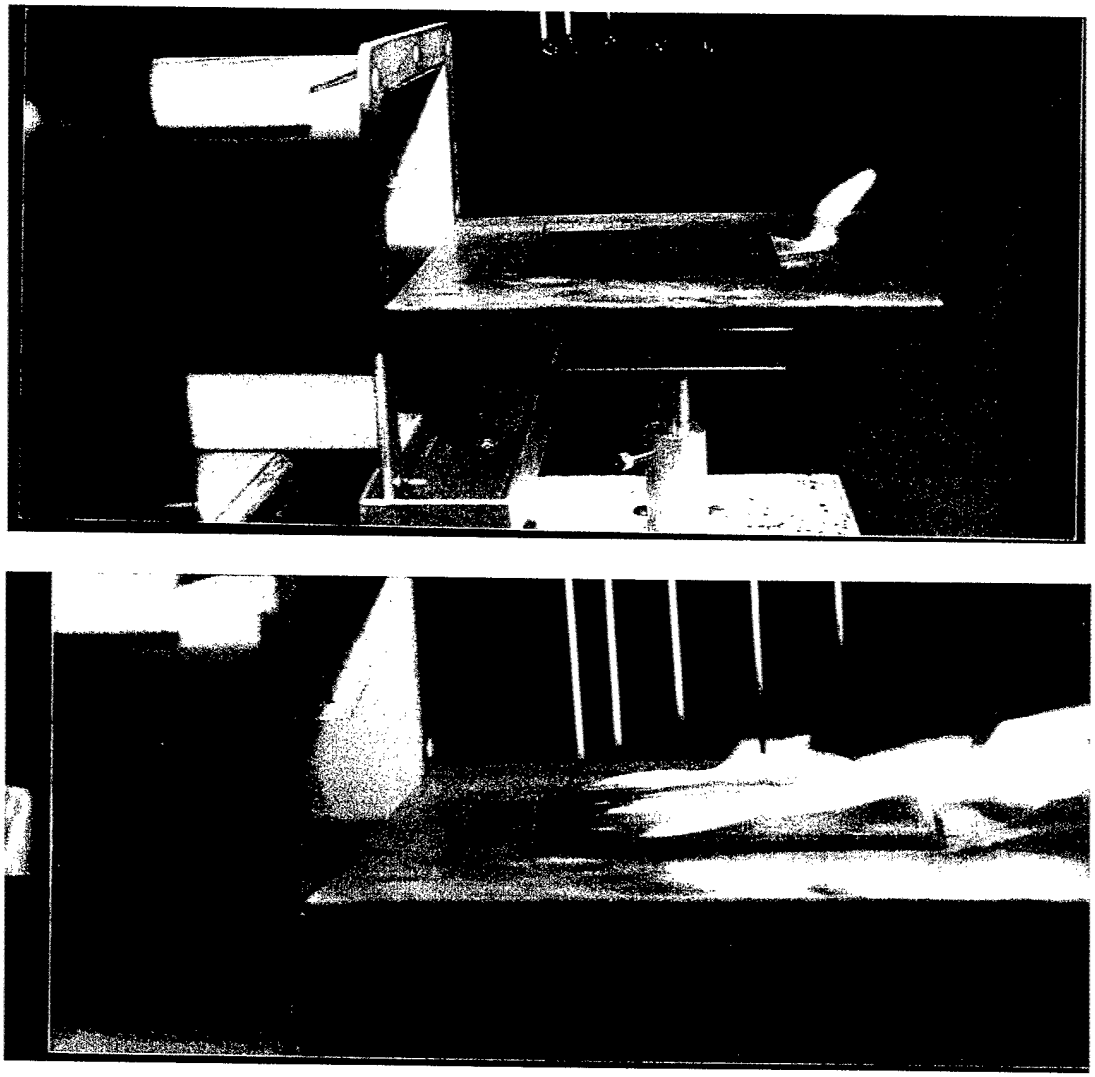

a

b

Figure 5: Effects of mist flow rate on the flame (a) high mist flow rate and is being blown off; (b) reduced mist flow rate flame is dislodged and a quench zone is formed

Figure 6: Burned surface profiles in the (a) Base case; (b) mist case (2_CFN4 @ 300 psi); (c) mist case (WDB1 @ 50 psi.)

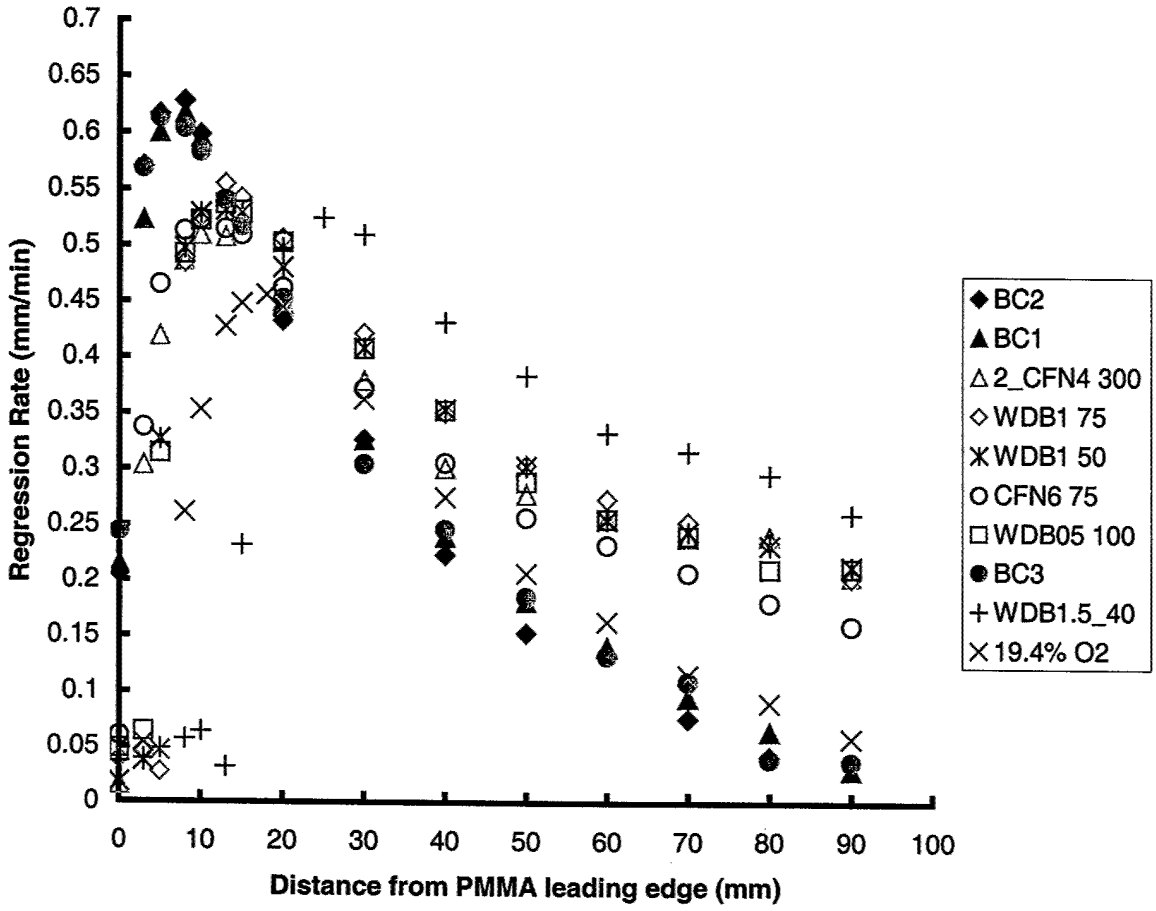

Figure 7: Variation of Surface regression rate with stream-wise location, X

tests. The initial quench zone is highest (~25 mm) in the test with the WDB1.5 nozzle and hence the suppression in burning rate in the leading section is highest in this test. In many cases the flame did not spread up to the sample leading edge within the 10-minute burn time. Thus, most spots within the initial quench zone were covered by flame for less than 10 minutes. Consequently the time-averaged (over 10 minutes) regression rate is less than the base case, where the flame covered the entire surface all the time.

In the downstream section (X > 30 mm) the local burning rate seems to have been enhanced by the addition of mist by as much as a factor of two. Indeed, the burning rate is enhanced by more than a factor of two with WDB1.5 nozzle at 40 psi. This result seems strange. Figure 7 also shows data with 19.4% oxygen. In this test instead of mist we added additional nitrogen to the airflow to reduce the oxygen concentration to 19.4%. Because of the nitrogen dilution we had an initial quench zone of ~ 20 mm and consequently, a substantial suppression in local burning rate in the leading section. However unlike the mist cases the burning rate was not enhanced downstream. It was observed (visually) that the flames in the tests with mist are more turbulent that the base case or nitrogen case flames. This will be discussed in more details later.

Next, we compare the temperature profiles with and without mist (Figs.8 and 9) at various stream-wise locations, X. Again, the solid symbols are base case data, while the open symbols are mist case data. Figure 8 shows two temperature profiles downstream, at X = 55 and X =75 mm. Recall that the sample length is 95 mm. The figure shows the following features. First, in the downstream section (especially, X > 50 mm) the effects of mist seem to have suppressed the gas phase temperature on the airside of the diffusion flame (right side of the peak temperature) but enhanced it on the fuel side. Secondly, the flame standoff distance, δ, which is approximated as the height at the temperature peak location, is less with mist than without mist. For example, at X= 75 mm, δ ~ 9 mm without mist and ~ 6 mm with mist. Finally, the temperature gradient seems to be higher with mist (qualitatively) on the fuel side of the flame. It therefore implies that downstream, the heat feedback to the sample surface, which is proportional to $\Delta T/\delta$, went up with the addition of fine water mist. Thus, the burning rate would increase, consistent with what we showed in Fig. 7. By comparing the profiles in Figs. 8 and 9 we note that these effects seem to progressively increase as X increases, just like the burning rate is further enhanced as X increases in Fig 7. Also plotted in Fig. 8 (the "x" symbol) are temperature profiles in the test with additional nitrogen. These data do not show similar tend as the mist data. Rather, they are close to the base case data, implying that the heat feedback was not enhanced downstream. This is also consistent with the burning rate results.

Furthermore, the total burning rate was numerically estimated by summing up the local burning rates. The results are shown in Table 2, for the base case, nitrogen case and various mist cases. Table 2 shows that in the base case tests, the total burning rate was ~ 1.8 gm/min, with half of it coming from the first 20 mm of the sample. However, with the mist cases, the total burning rate jumped to ~ 2.5 gm/min, with about 70% of it coming from X > 20 mm. With nitrogen, on the other hand, the total burning rate decreased to ~1.7 gm/min, with most of it coming from downstream. These results suggest that the observed enhancement in burning rate by water mist is real.

It is not very clear why the addition of mist would lead to increased local burning rate in the trailing section. However, one could speculate that the introduction of mist increased turbulence in the airflow. This was observed visually and temperature profiles showed a lot more wrinkles (especially downstream) with mist than without mist. The effects of turbulence would increase mixing, which would enhance combustion as well as bring the flame closer to the

surface. Indeed, δ decreased with the addition of mist especially downstream (Fig. 8). Indeed, the effects of turbulence on the burning rate of PMMA in a boundary layer configuration were studied by Zhou and Fernandez-Pello [26]. They mechanically induced turbulence in the airflow without mist and showed that the local normalized burning rate $\propto$ (turbulence intensity)$^{0.5}$. Thus, doubling the turbulence intensity would enhance the burning by ~ 40%.

Our speculation that mist induced turbulence played a significant role in the burning rate enhancement is supported by a comparison of the data with mist, where we had turbulence and the data with nitrogen dilution, where we had no turbulence (Figs. 7 and 8). With nitrogen dilution, the gas phase temperature profiles are smooth like the base case profiles (Fig.8) and the flame was not observed to be turbulent. Also, with nitrogen, the temperature data in Fig. 8 show no significant increase in temperature or temperature gradient on the fuel side of the diffusion flame, unlike in the mist cases. Finally, the burning rate showed a greater suppression in the leading section but no significant enhancement down stream in the tests with nitrogen (Fig. 7). Therefore, it is likely that mist induced turbulence contributed significantly to the observed enhancement in burning rate. More detailed tests will be conducted to confirm this. It is also necessary to determine whether turbulence is induced by the spraying activity at the nozzle location and/or the evaporation of droplets in the flame.

Mist enhanced burning rate was also observed by Atreya et al [27] in their work with methane diffusion flames. They ran experiments, where liquid water was introduced on the surface of a methane ceramic burner. With a sooty methane flame, they observed an increase in heat release rate at low water application rates and suppression in heat release rate at high water application rates. However, they did not observe similar effects in a blue methane flame. To determine whether the enhancement is as a result of chemical effects or as a result of increased mixing due to the volumetric changes during droplet evaporation, they ran further experiments with methane counter-flow diffusion flames, where water vapor was introduced with the air. Their results show that as water vapor replaced nitrogen in the air, the heat release rate went up. This suggests that water vapor at low concentrations may enhance the combustion reactions, perhaps through the water gas reaction.

Finally, the observed effects of mist addition in the current tests suggest that mist droplets did not reach the pyrolyzing fuel surface in significant numbers, and the effects of surface cooling were insignificant. Our earlier work with pool fires [13] showed that significant suppression is obtained with high boiling point fuels when the droplets can reach the surface. With free stream velocity of 84 cm/s and mean droplet diameters in the range of 50 μm, it seems that the droplets evaporated in the hot flame gas layer in the current experiments. This speculation is supported by recent results of numerical simulations by Ananth et. al [28], which shows that with 60 μm diameter mono-disperse droplets, mist droplet concentration a few mm above the burning PMMA surface is zero. If the droplets cool the surface directly, the surface temperature will decrease rapidly and the pyrolysis rate will decrease significantly since the pyrolysis rate decreases exponentially with temperature.

Table2: Estimated total burning rates in tests with and without mist.

Test Condition	Total Estimated burning rate (gm/min)	Burning rate in first 20 mm (gm/min)	Burning rate beyond 20 mm (gm/min)
BC1	1.88	0.917	0.963
BC2	1.78	0.923	0.857
BC3	1.91	0.966	0.914
2_CFN4 _300	2.49	0.794	1.696
WDB1_50	2.54	0.747	1.793
WDB05_100	2.52	0.761	1.759
WDB1.5_40	2.58	0.318	2.262
CFN6_75	2.38	0.838	1.542
19.4% O2 (Add'l N2)	1.69	0.551	1.139

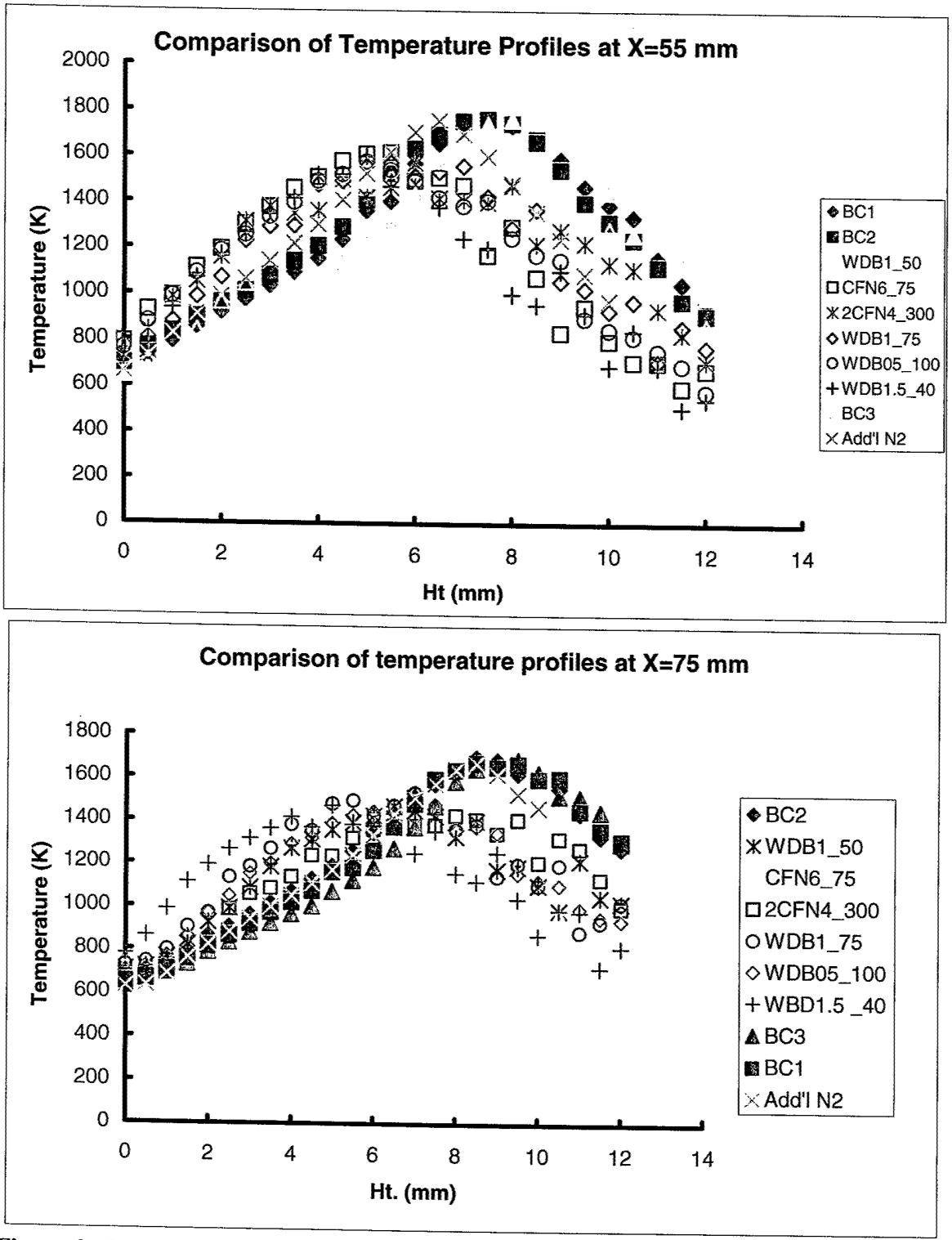

Figure 8: Comparison of temperature profiles in the downstream section.

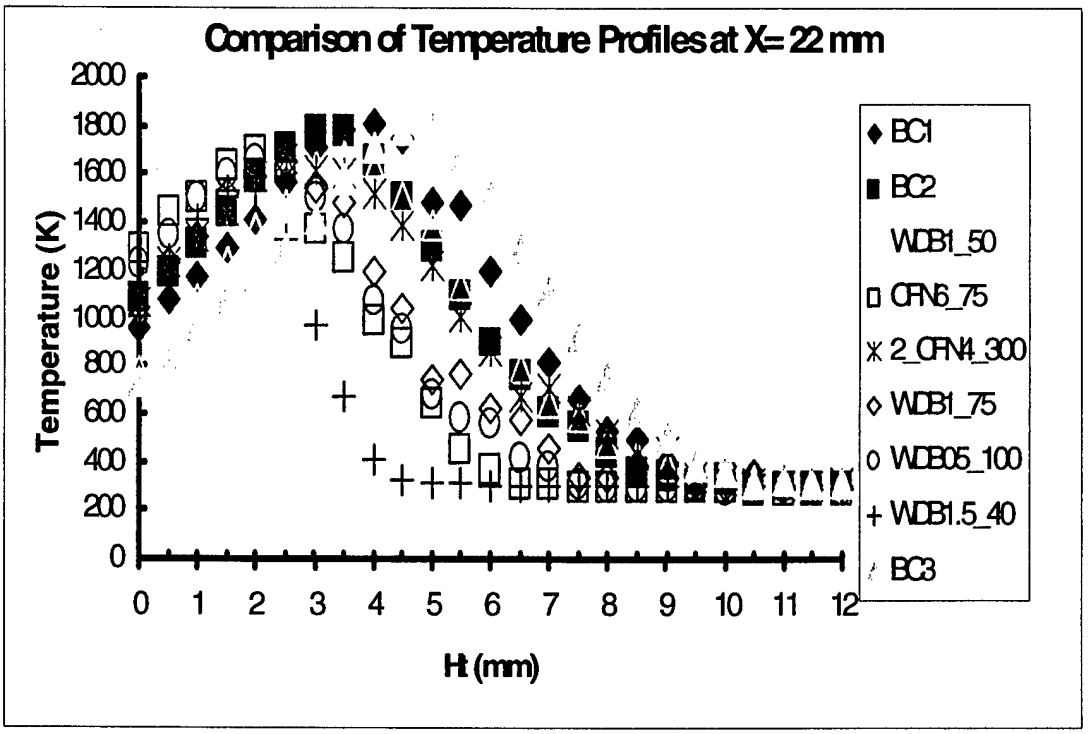

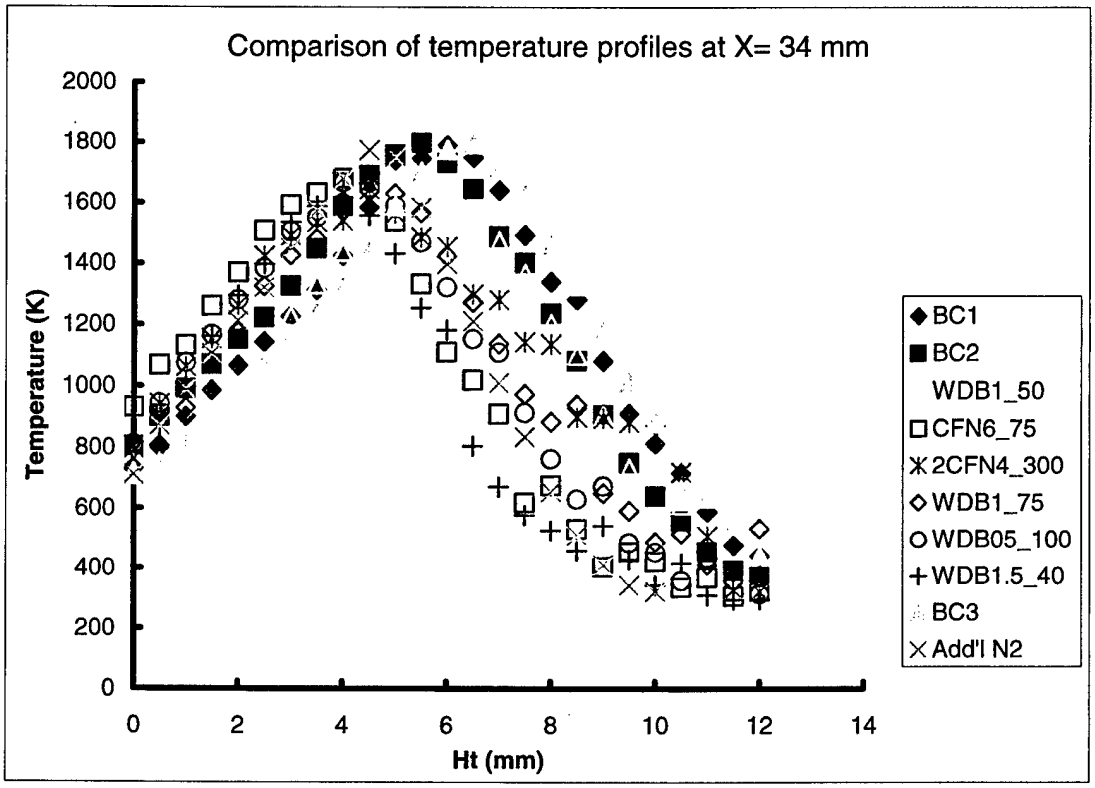

Figure 9: Comparison of temperature profile in the leading section

4.0 SUMMARY

In the preceding section we presented preliminary results on the investigation of the effects of water mist on the burning of a forced convection boundary layer flame over

PMMA. Fine water spray (SMD < 100 μm) was introduced with the incoming airflow at U_∞ = 84 cm/s. The time-averaged local burning rates were measured and gas phase temperature profiles were mapped with and without water mist. Analysis of the results shows the following trends:

1. Flame extinguishment is obtained by the creation of a quench zone in the leading section and subsequent flame blow off instead of by the cooling and shrinking of the flame.

2. At the current experimental conditions, the introduction of mist seems to induce turbulence and this enhances heat feedback to the condensed fuel and this resulted in the increase in the local burning rate, especially downstream.

3. Finally, the results suggest that at these conditions fuel surface cooling by mist droplets' evaporation on the surface is not significant.

This work is still in progress. Full mist characterization tests will be completed and further tests will be run where mist flow rate, air inlet velocity and test time will be varied. We suspect that turbulence is induced in these tests by the injection of mist with nozzles. Therefore, other mist generation tools (e.g. ultrasonic mist generator) will be tested to eliminate the effects of nozzle-induced turbulence.

5.0 ACKNOWLEDGEMENTS:

The contributions of Mr. Clarence Whitehurst in the experiments are hereby acknowledged. This work was funded by the office of Naval Research, through the Naval Research Laboratory, S&T Core Program.

6.0 REFERENCES:

1. Rasbash, D.J., Rogowski, Z.W., and Stark, G.W.V. " Mechanism of extinction of liquid fires with water sprays" *Combustion and Flame*, 4 :223 (1960)

2. Rasbash, D.J., and Rogowski, Z.W "Extinction of fires in liquids by cooling with water sprays," *Combustion and Flame*, 1 :4, (1957)

3. Rasbash, D.J. "The Extinction of fires by water sprays," *Fire Research Abstracts and Reviews*, 4 (1&2): 28, (1962)

4. Downie, B, Polmeropoulos, C and Gogos G. "Interaction of a water mist with a buoyant methane diffusion flame" *Fire Safety J.* **24** p.359 (1995)

5. Takahashi, S. "Extinguishment of plastic fires with plain water and wet water" *Fire Safety J.* **22** p.169 (1994)

6. McCaffrey B.J "Jet Diffusion Flame Suppression using water Sprays - An Interim report" *Comb. Sci. and Tech.* **40** p.107 (1998)

7. Alpert R; "Calculated interaction of spray with large scale buoyant flows" *J. Heat Transfer* **105** p.310 (1984)

8. Bill R.G; "Numerical simulation of actual delivered density (ADD) measurements" *Fire Safety J.* **20** p.227 (1993)
9. Prasad, K; Li, C; Kailasanath, K; Ndubizu, C; Ananth R and Tatem P.A; "Numerical modeling of water mist suppression of methane-air diffusion flame" *Comb. Sci. & Tech.* **132** 1-6 p.325 (1998)

10. Prasad, K; Li, C; Kailasanath, K; Ndubizu, C; Ananth R and Tatem P.A; "Numerical modeling of fire suppression using water mist - 2. Methanol liquid pool fires" NRL Memorandum report NRL/mr/6410-98-8190 (1998)

11. Prasad, K; Li, C; Kailasanath, K; Ndubizu, C; Ananth R and Tatem P.A; "Numerical modeling of methanol Liquid pool fires for fire suppression" Annual Conference on Fire Research, National Institute of Standards and Technology, Gaithersburg, MD Nov. 2-5 1998 NISTIR 6242 p.69

12. Ndubizu, C.C, Ananth, R. and Tatem, P.A "The effects of Droplet Size and Injection Orientation on Water Mist Suppression of Low and High Boiling point Liquid Pool Fires" *Comb. Sci. and Tech* **157** pp 63 (2000)

13. Ndubizu, C.C; Ananth,R.; Tatem, P.A; and Motevalli, V; "On Water mist fire suppression mechanisms in a gaseous diffusion flame" *Fires Safety J.* **31:3** p.253 (1998)

14. Tamanini F; "A study of the extinguishments of vertical wood slabs in self-sustained burning by water spray application" *Combust. Sci. and Tech,* **14** p.1 (1976)

15. Magee R .S and Reitz R. D "Extinguishment of radiation augmented plastic fires by water mist" *Proc. Comb. Inst.* **15** pp.337

16. Ndubizu, C.C, Ananth, R. and Tatem, P.A "The burning of a thermoplastic material under a forced-flow boundary layer flame" NRL Memorandum report NRL/mr/6180-02-8630 (2002)

17. Ndubizu, C.C, Ananth, R. and Tatem, P.A "Boundary layer flame spread over PMMA within the quench zone: A moving boundary effect" *Combust. Sci. Tech.* (In press)

18. McAlevy R.F and Magee R.S "The mechanism of flame spreading over the surface of igniting condensed-phase materials" *Proc. Comb. Inst.* **12**:215. (1969)

19. duPlessis, M.P; Wang, R.L and Kahawita R "Investigation of the near-region of a square jet" *J. Fluid Eng.* **96** p.246-251 (1974)

20. Sfeir, A.A "The velocity and temperature fields of rectangular jets" *Int. J Heat Mass Transfer* **19** p.1289-1297 (1976)

21. Sforza, P.M; Streiger, M.H and Trentacoste N " Studies of three-dimensional viscous jets" *AIAA J.* **4** No.5 p.800 (1966)

22. Vovelle, C: Akrich R; Delfau J.L and Gresillaud S. "Influence of the thickness on the thermal degradation of PMMA" *Fire Safety Science: Proceedings of the first International Symposium,* Hemisphere. Washington D.C pp. 473. (1986)

23. Tewarson, A. and Pion R.F., "Flammability of plastics – I Burning intensity" *Combust. Flame* **26** :85 (1976)

24. Krishnamurthy L. and Williams F.A "Laminar combustion of poly methylmethacrylate in O_2/N_2 mixtures" *Proc. Comb. Inst.* **14** *pp.1151 (1974)*

25. The Temperature Handbook, Vol. 29; Omega Engineering Inc. pp. Z159. (1995)

26. Zhuo L and Fernandez-Pello A.C "Turbulent burning of a flat fuel surface" *Fire Safety Science: Proceedings of the third International Symposium,* Hemisphere. Washington D.C pp. 414-424 (1990)

27. Atreya A., Crompton T. and Suh J. "An Experimental and theoretical study of mechanisms of fire suppression by water" Proceedings of NIST Annual conference on fire research, NISTIR 5499 pp.67 (1994)

28. Ananth,R.; Ndubizu, C.C; Tatem, P.A "Dynamics of suppression of a boundary layer flame formed over a solid surface with forced flow of air containing water mist" Proceedings of the third Joint Meeting of the U.S Sections of The Combustion Institute, Chicago Il. March 16-19 (2003)

APPENDIX

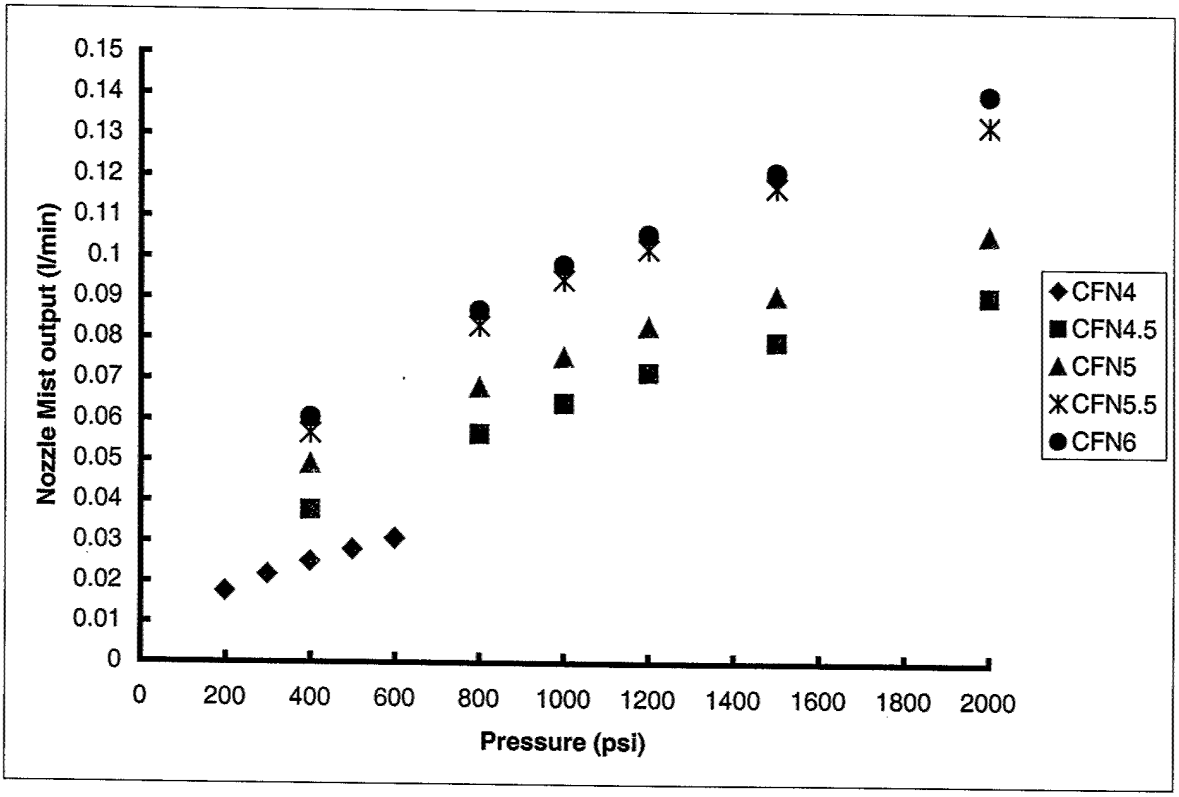

Figure A1: Variation of Mist output with water pressure for the various nozzles